Supporting Information

C-C Coupling Reactions Promoted by CNT-Supported Bimetallic Center in Fischer-Tropsch Synthesis

Chi-You Liu and Elise Y. Li*

Department of Chemistry, National Taiwan Normal University

No. 88, Section 4, Tingchow Road, Taipei 116, Taiwan

* Corresponding author E-mail: eliseytli@ntnu.edu.tw

* Corresponding author ORCID: 0000-0003-1206-1110

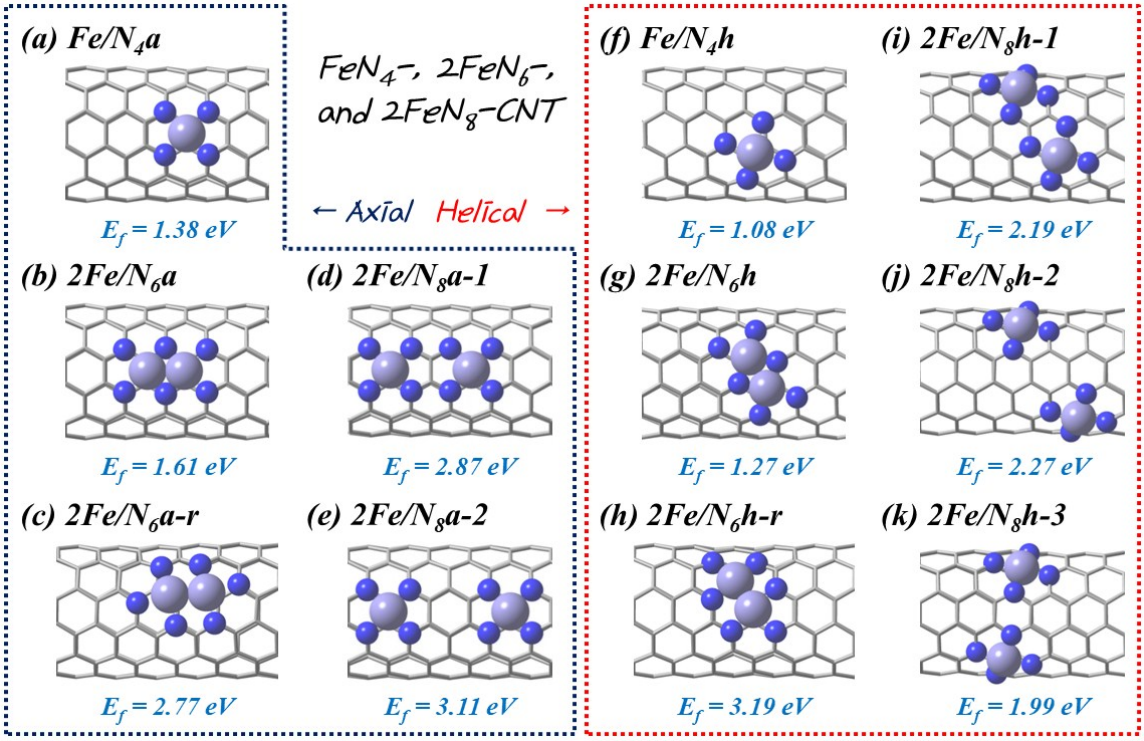

Figure S1. Optimized structures and the formation energies (E_f, in eV) of different single or bimetallic Fe decorated N-doped (6,6)-CNT surfaces along the (a-e) axial or (f-k) helical directions. The colors of the elements N, C, and Fe are blue, gray, and purple, respectively.

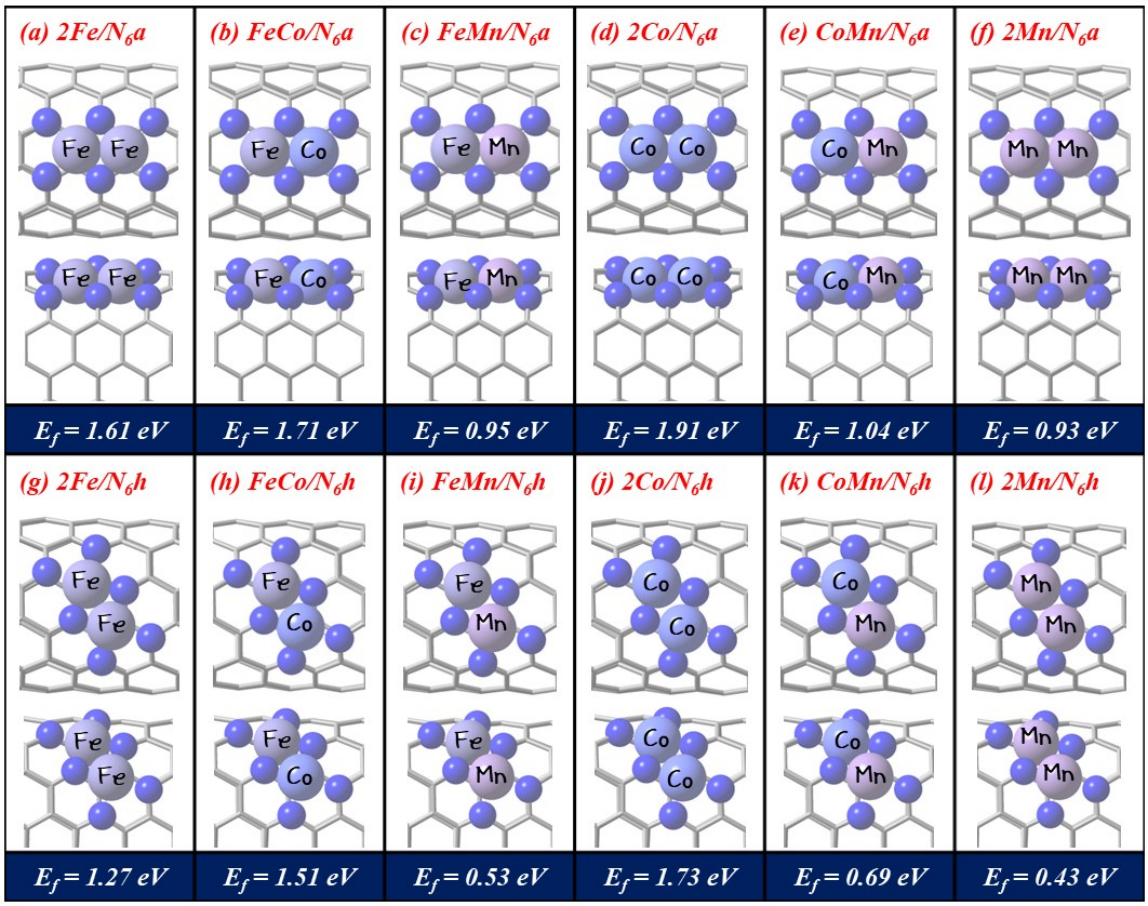

Figure S2. Optimized structures and the formation energies (E_f, in eV) of different bimetallic centers on (a-f) N_6a and (g-l) N_6h surfaces.

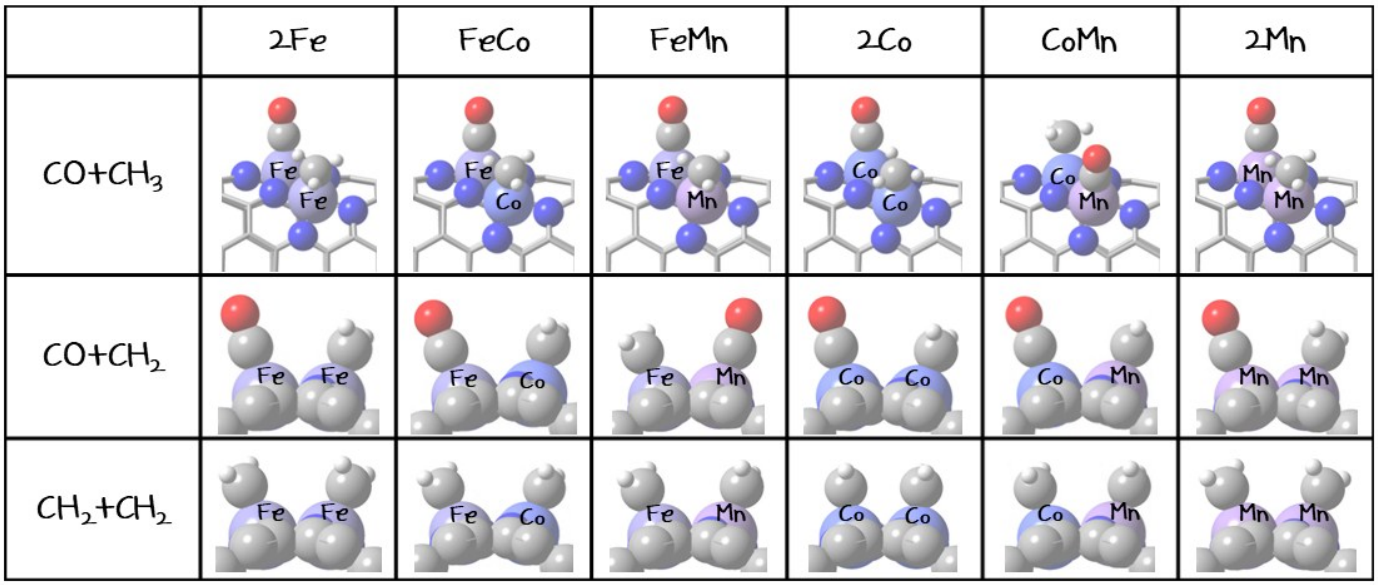

Figure S3. Optimized structures of the [CO + CH_3], the [CO + CH_2], and the [CH_2 + CH_2] co-adsorption on different M_1M_2/N_6h surfaces.

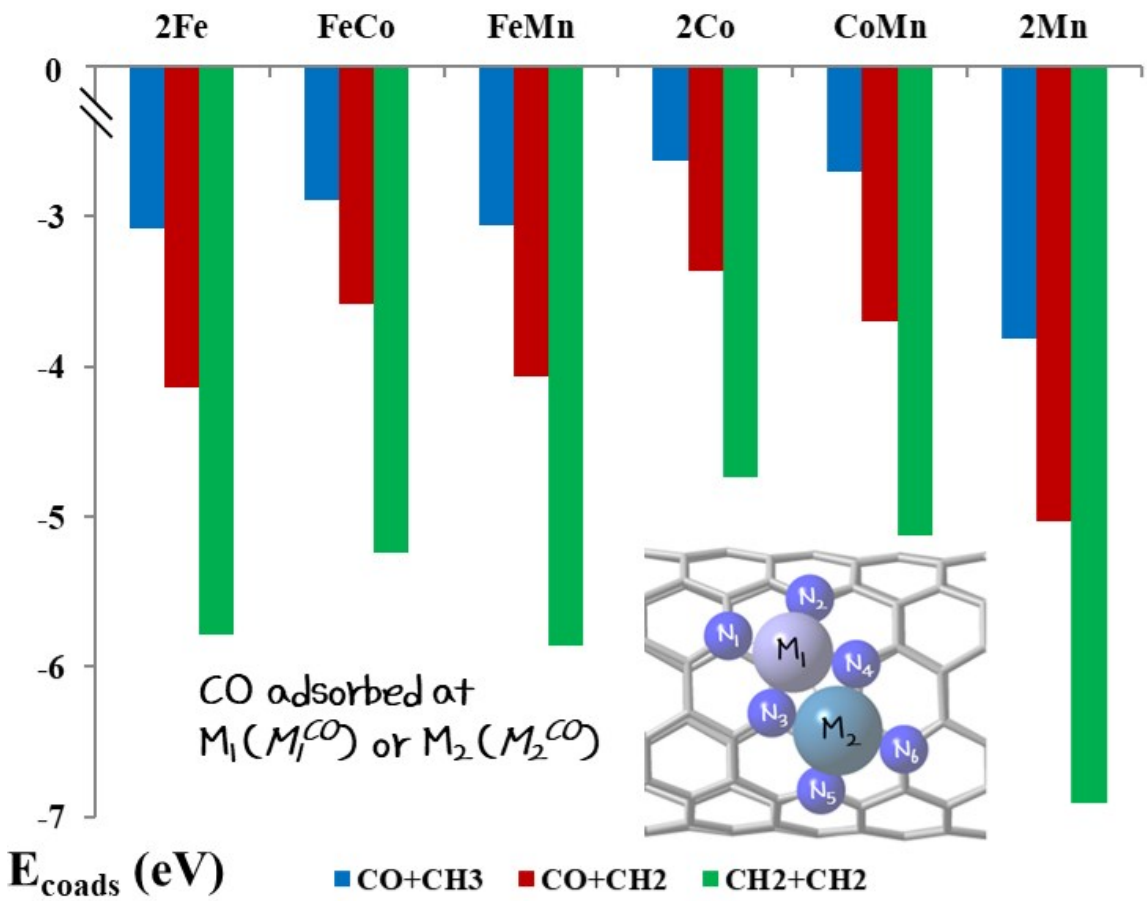

Figure S4. The co-adsorption energies (E_{coads}, in eV) of the [CO + CH_3], the [CO + CH_2], and the [CH_2 + CH_2] on different M_1M_2/N_6h surfaces. The labels of N, M_1, or M_2 are plotted in the figure. M_1^{CO} or M_2^{CO} represents the adsorption of CO on the M_1 or M_2 site, respectively.

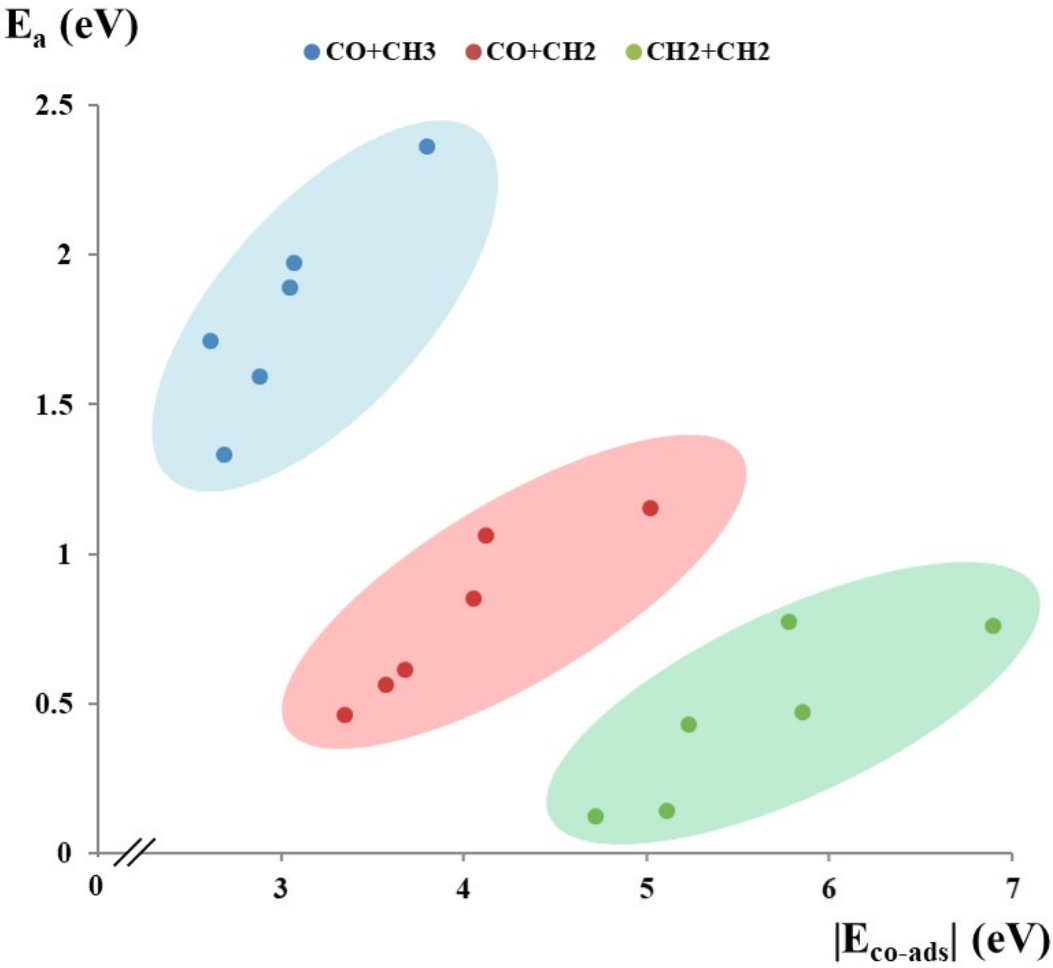

Figure S5. The correlation of E_a and $|E_{coads}|$ for the [CO + CH_3], the [CO + CH_2], and the [CH_2 + CH_2] reactions on M_1M_2/N_6h surfaces.

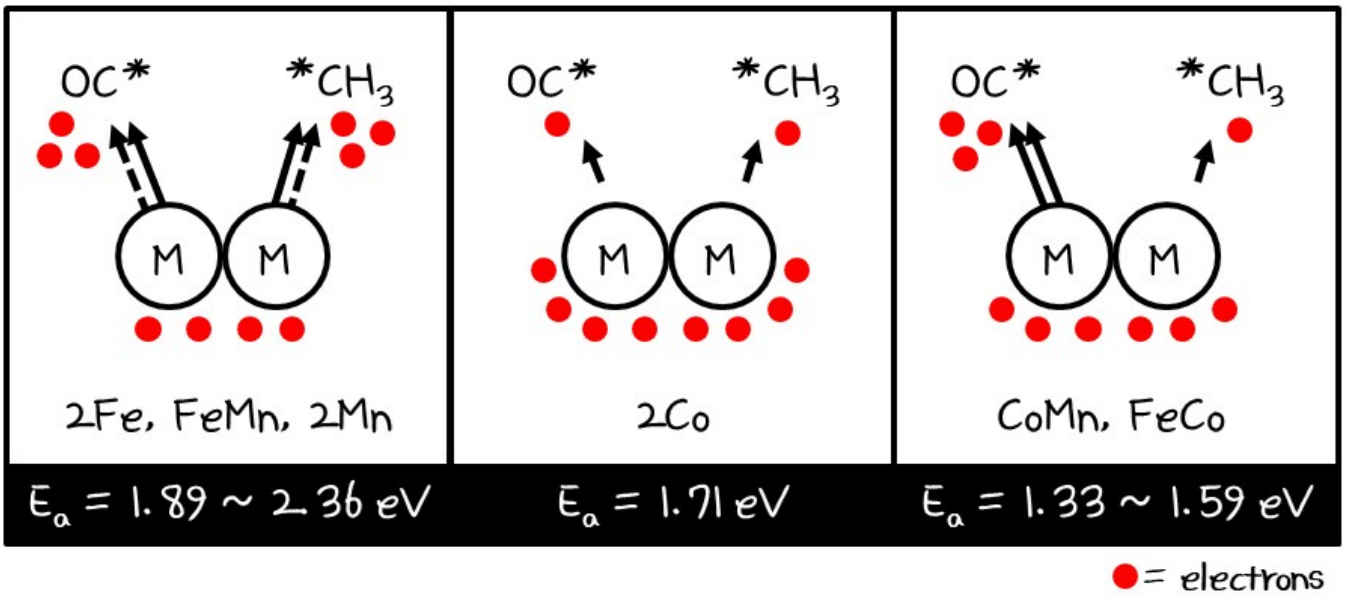

Figure S6. Schematic representation of different extent of electron transfer for the [CO + CH_3] adsorbates on M_1M_2/N_6h surfaces.

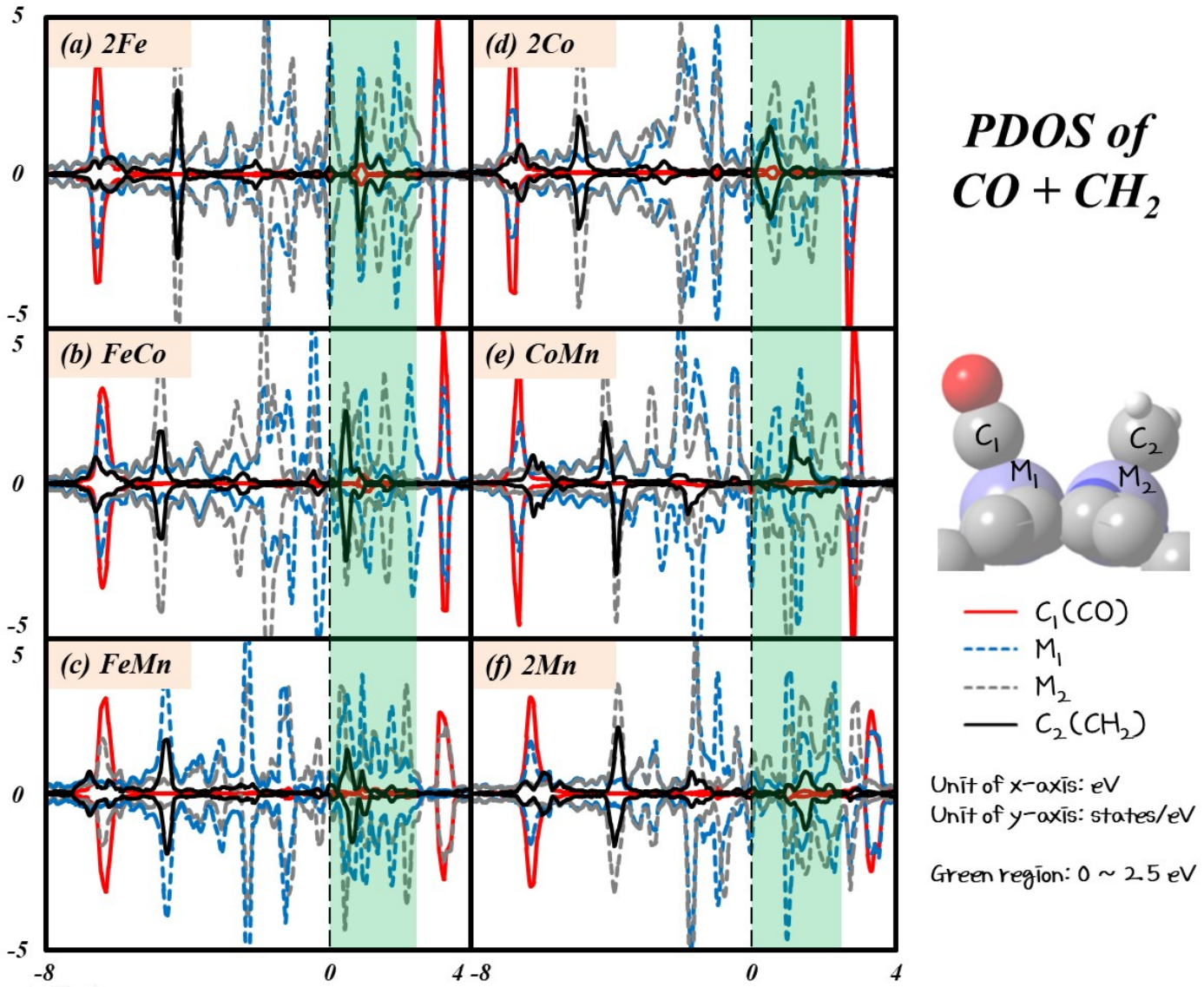

Figure S7. Partial density of states (PDOS) projection of the [CO + CH_2] adsorbed on the (a) 2Fe, (b) FeCo, (c) FeMn, (d) 2Co, (e) CoMn, and (f) 2Mn/N_6h surfaces. The energy is shifted with respect to Fermi level. The area E = 0 ~ 2.5 eV is shaded in green. The colors of elements N, C, O, and H are blue, gray, red, and white, respectively.

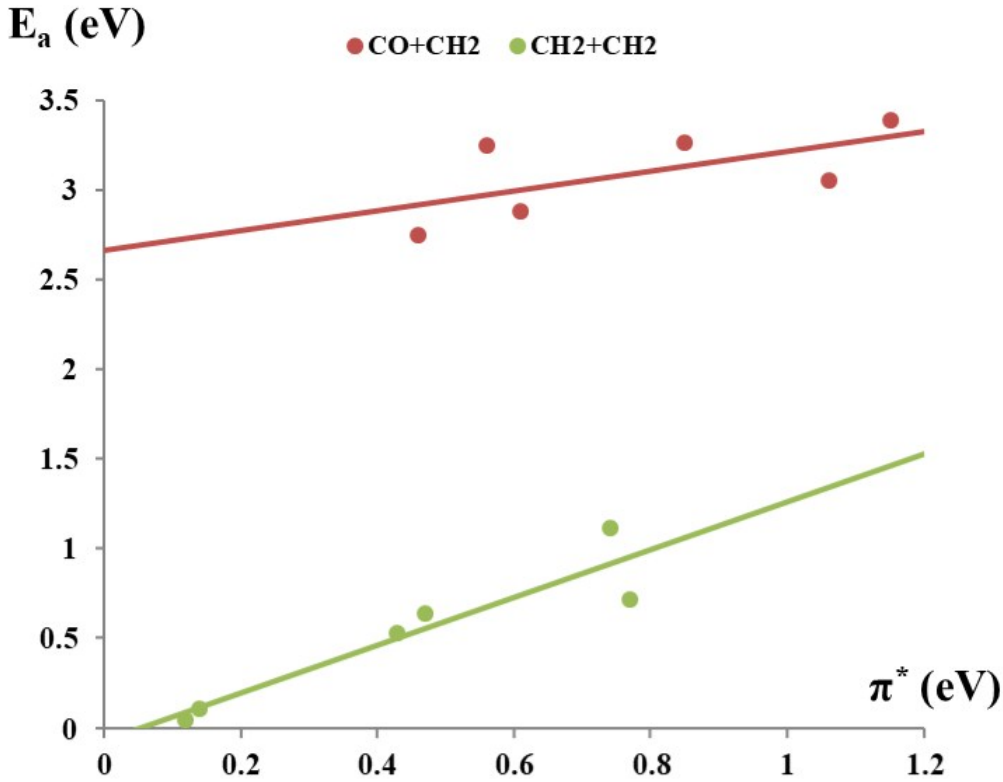

Figure S8. The correlation of E_a and π^* for the [CO + CH_2] and the [CH_2 + CH_2] reactions on the M_1M_2/N_6h surfaces.

Table S1. The co-adsorption energies (E_{coads}, in eV) of adsorbates on the M_1M_2/N_6h surfaces. The $M_{1/2}^{CO}$ represents the adsorption of CO at the M_1 or M_2 metal site.

M_1M_2	Sites	CO+CH_3	CO+CH_2	CH_2+CH_2
2Fe	M_1^{CO}=M_2^{CO}	-3.08	-4.13	-5.78
FeCo	M_1^{CO}	-2.89	-3.58	-5.24
	M_2^{CO}	-2.63	-3.80	
FeMn	M_1^{CO}	-3.06	-4.21	-5.86
	M_2^{CO}	-3.16	-4.06	
2Co	M_1^{CO}=M_2^{CO}	-2.62	-3.36	-4.73
CoMn	M_1^{CO}	-2.52	-3.69	-5.12
	M_2^{CO}	-2.70	-3.24	
2Mn	M_1^{CO}=M_2^{CO}	-3.81	-5.03	-6.90

Table S2. The migration pathways, activation energies (E_a, in eV), reaction energies (ΔE, in eV), and the final state energies (E_P, in eV) of the [**CO + CH_3 → $COCH_3$**] reaction on the M_1M_2/N_6h surfaces. The migration direction is denoted by the arrow.

M_1M_2	Pathways	E_a	ΔE	E_p
2Fe	$M_1^{CO\leftarrow}=M_1^{CO\rightarrow}$	**1.97**	**-0.14**	**-0.14**
FeCo	$M_1^{CO\leftarrow}$	**1.59**	**-0.38**	**-0.38**
	$M_1^{CO\rightarrow}$	2.23	+0.19	+0.19
	$M_2^{CO\rightarrow}$	1.87	-0.61	-0.35
	$M_2^{CO\leftarrow}$	2.02	-0.15	+0.11
FeMn	$M_1^{CO\leftarrow}$	**1.89**	**-0.16**	**-0.06**
	$M_1^{CO\rightarrow}$	1.95	+0.10	+0.20
	$M_2^{CO\rightarrow}$	2.51	+0.26	+0.26
	$M_2^{CO\leftarrow}$	2.12	+0.09	+0.09
2Co	$M_1^{CO\leftarrow}=M_1^{CO\rightarrow}$	**1.71**	**-0.53**	**-0.53**
CoMn	$M_1^{CO\leftarrow}$	1.87	-0.13	+0.05
	$M_1^{CO\rightarrow}$	1.62	-0.58	-0.40
	$M_2^{CO\rightarrow}$	2.28	+0.09	+0.09
	$M_2^{CO\leftarrow}$	**1.33**	**-0.44**	**-0.44**
2Mn	$M_1^{CO\leftarrow}=M_1^{CO\rightarrow}$	**2.36**	**+0.14**	**+0.14**

Table S3. The co-adsorption sites, activation energies (E_a, in eV), reaction energies (ΔE, in eV), and the final state energies (E_P, in eV) of the [**$CO + CH_2 \rightarrow COCH_2$**] as well as the [**$CH_2 + CH_2 \rightarrow (CH_2)_2$**] reactions on the M_1M_2/N_6h surfaces.

M_1M_2	Sites	E_a	ΔE	E_P	M_1M_2	E_a	$\Delta E=E_P$
$CO + CH_2 \rightarrow COCH_2$					**$CH_2 + CH_2 \rightarrow (CH_2)_2$**		
2Fe	$M_1^{CO}=M_2^{CO}$	**1.06**	**-0.44**	**-0.44**	2Fe	**0.77**	**-2.08**
FeCo	M_1^{CO}	**0.56**	**-0.82**	**-0.59**	FeCo	**0.43**	**-2.43**
	M_2^{CO}	0.66	-0.73	-0.73			
FeMn	M_1^{CO}	0.90	-0.45	-0.45	FeMn	**0.47**	**-2.09**
	M_2^{CO}	**0.85**	**-0.47**	**-0.31**			
2Co	$M_1^{CO}=M_2^{CO}$	**0.46**	**-1.18**	**-1.18**	2Co	**0.12**	**-2.92**
CoMn	M_1^{CO}	**0.61**	**-0.73**	**-0.73**	CoMn	**0.14**	**-2.39**
	M_2^{CO}	0.53	-0.73	-0.28			
2Mn	$M_1^{CO}=M_2^{CO}$	**1.15**	**-0.03**	**-0.03**	2Mn	**0.74**	**-1.44**

Table S4. The Bader charge populations (q, in |e|) of the M_1M_2/N_6h surfaces. The labels of the atoms refer to Figure S4.

M_1M_2	$q(M_1)$	$q(M_2)$	$q(N_1)$	$q(N_2)$	$q(N_3)$	$q(N_4)$	$q(N_5)$	$q(N_6)$
2Fe	+1.28	+1.28	-2.51	-2.59	-1.98	-2.03	-2.59	-2.61
FeCo	+1.30	+1.00	-2.48	-2.58	-1.94	-1.88	-2.54	-2.56
FeMn	+1.24	+1.57	-2.48	-2.58	-2.03	-2.10	-2.61	-2.63
2Co	+1.05	+1.04	-2.57	-2.67	-1.97	-1.94	-2.56	-2.57
CoMn	+0.97	+1.60	-2.45	-2.54	-1.98	-2.02	-2.62	-2.65
2Mn	+1.51	+1.45	-2.62	-2.59	-2.07	-2.13	-2.61	-2.63

Table S5. The Bader charge population difference (Δq, in |e|) before and after the adsorption of different adsorbates (A_1 and A_2) on the M_1M_2/N_6h surfaces.

M_1M_2	$\Delta q(M_1)$	$\Delta q(M_2)$	$\Delta q(A_1)$	$\Delta q(A_2)$
		CO + CH_3		
2Fe	+0.11	+0.13	-0.26 (CO)	-0.17 (CH_3)
FeCo	+0.11	+0.14	-0.29 (CO)	-0.10 (CH_3)
FeMn	+0.12	+0.13	-0.27 (CO)	-0.26 (CH_3)
2Co	+0.09	+0.09	-0.18 (CO)	-0.08 (CH_3)
CoMn	+0.14	+0.06	-0.08 (CH_3)	-0.38 (CO)
2Mn	+0.09	+0.20	-0.36 (CO)	-0.24 (CH_3)
		CO + CH_2		
2Fe	+0.12	+0.17	-0.27 (CO)	-0.24 (CH_2)
FeCo	+0.11	+0.17	-0.28 (CO)	-0.11 (CH_2)
FeMn	+0.16	+0.07	-0.18 (CH_2)	-0.37 (CO)
2Co	+0.14	+0.09	-0.18 (CO)	-0.12 (CH_2)
CoMn	+0.12	+0.18	-0.17 (CO)	-0.34 (CH_2)
2Mn	+0.08	+0.21	-0.36 (CO)	-0.34 (CH_2)
		CH_2 + CH_2		
2Fe	+0.17	+0.16	-0.23	-0.23
FeCo	+0.16	+0.16	-0.24	-0.10
FeMn	+0.19	+0.17	-0.22	-0.36
2Co	+0.12	+0.13	-0.13	-0.12
CoMn	+0.18	+0.17	-0.12	-0.34
2Mn	+0.12	+0.19	-0.34	-0.35

Table S6. Reported theoretical values of the barriers (E_a, in eV) of the three C-C coupling reactions catalyzed by **2Co/N_6h-CNT, CoMn/N_6h-CNT**, and other catalysts in FTS.

Catalysts	$CO + CH_3$	$CO + CH_2$	$CH_2 + CH_2$	Reference
Fe(111)	1.05	1.35	1.06	[1]
χ-Fe_5C_2(510)	1.35	1.16	1.03	[2]
Co(111)	1.37	0.69	0.42	[3]
Co(0001)	1.19	0.56	0.12	[4]
Co(10-11)	1.50	1.00	0.47	[5]
Co(10-10)	1.17	0.60	0.33	[6]
Co_2C(101)	1.18	0.99	0.73	[7]
Co_2C(011)	0.46	0.87	0.55	[8]
C-Co_2C(101)	0.94	0.60	0.42	[9]
2Co/N_6h-CNT	**1.71**	**0.46**	**0.12**	**This work**
CoMn/N_6h-CNT	**1.33**	**0.61**	**0.14**	**This work**

Reference

(1) Li, H. J.; Chang, C. C.; Ho, J. J. Density Functional Calculations to Study the Mechanism of the Fischer-Tropsch Reaction on Fe(111) and W(111) Surfaces. *J. Phys. Chem. C* **2011**, *115*, 11045–11055.

(2) Pham, T. H.; Qi, Y.; Yang, J.; Duan, X.; Qian, G.; Zhou, X.; Chen, D.; Yuan, W. Insights into Hägg Iron-Carbide-Catalyzed Fischer-Tropsch Synthesis: Suppression of CH_4 Formation and Enhancement of C-C Coupling on χ-Fe_5C_2 (510). *ACS Catal.* **2015**, *5*, 2203–2208.

(3) Chen, C.; Wang, Q.; Wang, G.; Hou, B.; Jia, L.; Li, D. Mechanistic Insight into the C_2 Hydrocarbons Formation from Syngas on Fcc-Co(111) Surface: A DFT Study. *J. Phys. Chem. C* **2016**, *120*, 9132–9147.

(4) Qi, Y.; Yang, J.; Holmen, A.; Chen, D. Investigation of $C_1 + C_1$ Coupling Reactions in Cobalt-Catalyzed Fischer-Tropsch Synthesis by a Combined DFT and Kinetic Isotope Study. *Catalysts* **2019**, *9*, 551.

(5) Liu, H.; Zhang, R.; Ling, L.; Wang, Q.; Wang, B.; Li, D. Insight into the Preferred Formation Mechanism of Long-Chain Hydrocarbons in Fischer-Tropsch Synthesis on Hcp Co(10-11) Surfaces from DFT and Microkinetic Modeling. *Catal. Sci. Technol.* **2017**, *7*, 3758–3776.

(6) Zhang, R.; Kang, L.; Liu, H.; He, L.; Wang, B. Insight into the C-C Chain Growth in Fischer-Tropsch Synthesis on HCP Co(10-10) Surface: The Effect of Crystal Facets on the Preferred Mechanism. *Comput. Mater. Sci.* **2018**, *145*, 263–279.

(7) Zhang, R.; Wen, G.; Adidharma, H.; Russell, A. G.; Wang, B.; Radosz, M.; Fan, M. C_2 Oxygenate Synthesis via Fischer-Tropsch Synthesis on Co_2C and Co/Co_2C Interface Catalysts: How to Control the Catalyst Crystal Facet for Optimal Selectivity. *ACS Catal.* **2017**, *7*, 8285–8295.

(8) Wang, B.; Liang, D.; Zhang, R.; Ling, L. Crystal Facet Dependence for the Selectivity of C_2 Species over Co_2C Catalysts in the Fischer-Tropsch Synthesis. *J. Phys. Chem. C* **2018**, *122*, 29249–29258.

(9) Liu, P.; Liang, D.; Zhang, R.; Wang, B. The Formations of C_2 Species and CH_4 over the Co_2C Catalyst in Fischer-Tropsch Synthesis: The Effect of Surface Termination on Product Selectivity. *Comput. Mater. Sci.* **2020**, *172*, 109345.